A Preliminary Study of a Novel Heat Pump Integrated Underground Thermal Energy Storage for Shaping Electric Demand of Buildings

Xiaobing Liu[1], Liang Shi[2], Ming Qu[2], Joseph Warner[3]

[1]Oak Ridge National Laboratory, Oak Ridge, TN 37831, U.S.A.

[2]Purdue University, West Lafayette, IN 47906, U.S.A.

[3]University of Tennessee, Knoxville, TN 37996, U.S.A.

Keywords

flexible load, renewable power, thermal energy storage, dual-purpose underground thermal battery, heat pump, demand side management, modeling and simulation

ABSTRACT

A Dual-Purpose Underground Thermal Battery (DPUTB) innovatively integrates a ground heat exchanger with underground thermal energy storage. The DPUTB can be integrated with an Electric-Driven Heat Pump (EDHP) to enable more flexible electric load for meeting the thermal demands of a building (e.g., space cooling and space heating). A one-dimensional numerical model of the DPUTB is developed and validated against measured performance data of a small-scale DPUTB prototype. The validated DPUTB model is integrated with a heat pump model and a building energy simulation model to predict the load shifting performance and energy consumption of an integrated EDHP and DPUTB system. Preliminary simulation results indicate that the integrated system can flatten the electric load profile of a typical residential building and reduce the electric demand during peak hours by 37% on a typical summer day. In addition, the integrated EDHP and DPUTB system also reduces the daily power consumption of the building by 11% compared with a conventional residential space heating and cooling system.

1. Introduction

The increasing electricity generation from the renewable energy (solar, wind, etc.) in recent years raises challenge to the existing electric grid due to its intermittent characteristic. The 'duck curve' phenomenon shown in Fig. 1 reflects this mismatch between the renewable power supply and the demand from the grid. It will cause the electric generator working in an unstable condition which results in a lower efficiency and a shorter lifespan of the power plant. On the other hand, the increasing penetration of the renewable power generation would lead to excess power production during its peak generation period thus it has to be curtailed, this limits the use of the renewable power (NREL 2015).

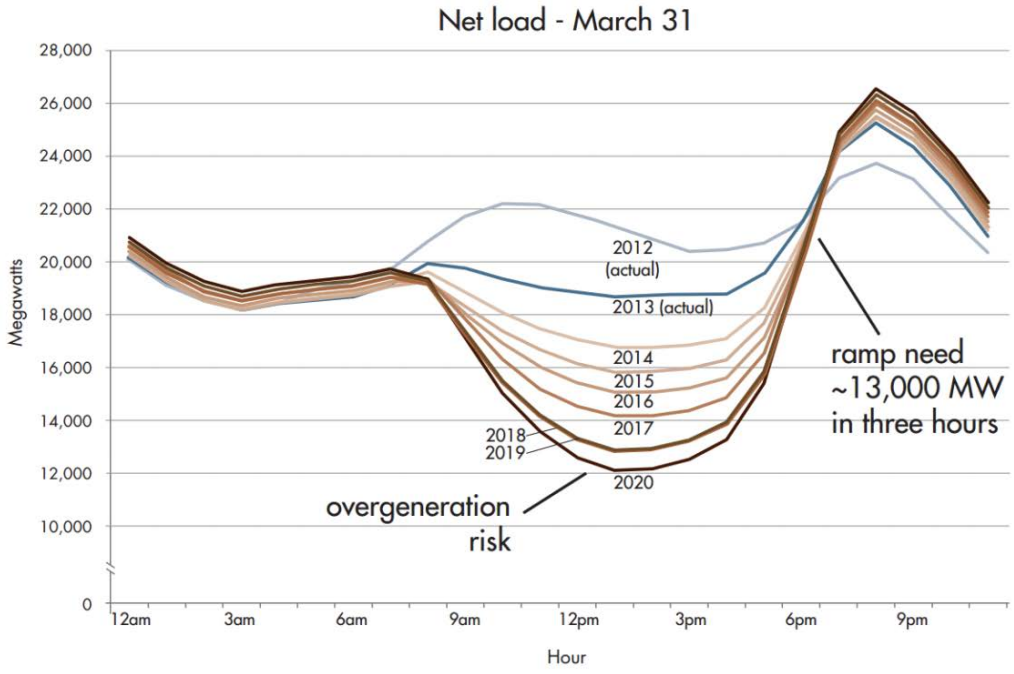

Fig. 1. 'Duck Curve' of electricity demand due to intermittent renewable power (CAISO 2013)

EIA reports (EIA 2018) that the heating, ventilation, and air-conditioning (HVAC) systems of commercial and residential buildings in the United States contribute about 20% to the total electricity consumption in the building section in 2017. The electric demand of buildings can be reshaped by shifting the thermal loads of the HVAC systems through thermal energy storage. A novel underground thermal energy storage technology, dual-purpose underground thermal battery (DPUTB), innovatively integrates a ground heat exchanger with underground thermal energy storage (Patent pending). As depicted in Fig. 2, the DPUTB consists of an enclosed inner tank within a larger water tank. A DPUTB stores thermal energy in its inner tank, and uses its outer annular body to exchange heat with the surrounding ground formation, in lieu of the ground heat exchanger of a ground source heat pump (GSHP). DPUTB can be installed in boreholes less than 6 m deep, costing much less than the conventional ground heat exchangers, which are usually installed in boreholes 60 meters deep. Customized phase change material (PCM) is wrapped on the outer surface of the inner tank. Because of the low thermal conductivity of the PCM, especially during the phase change process, the PCM serves as an insulation to block the heat transfer between the inner tank and the outer tank. In addition, the PCM also stores cooling or heating energy released from both tanks. Two heat exchangers are

installed in the inner and outer water tank, respectively, in order to exchange heat with a HVAC system. This design allows for storing chilled water or ice in the inner tank, which can provide direct cooling to eliminate the electricity consumption of the heat pump during the peak hours of the electric grid. The annulus of the DPUTB (space below the inner and outer tanks) can be used to exchange heat with the surrounding ground formation.

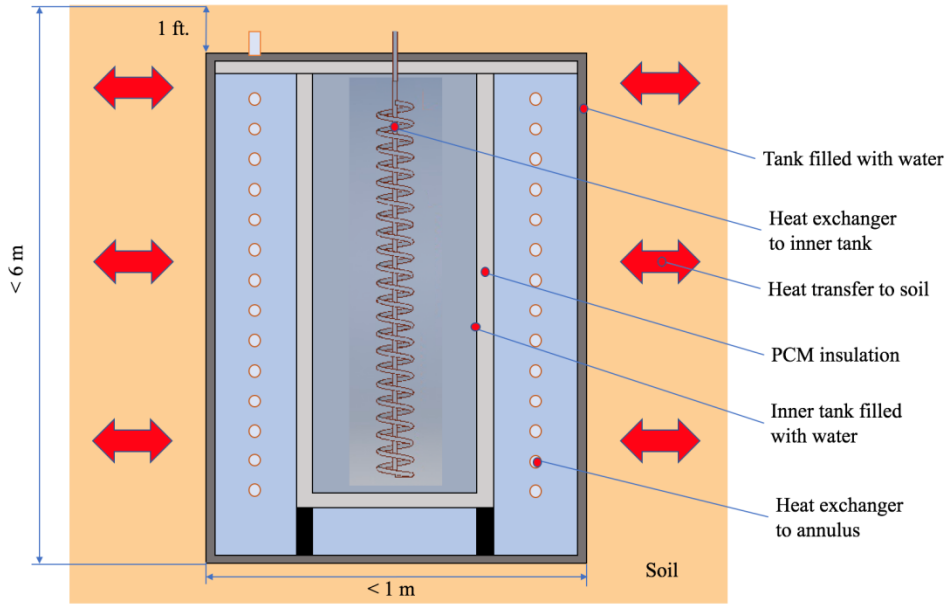

Fig. 2. Schematic of the dual-purpose underground thermal battery (Patent pending)

Combining the DPUTB with a dual-source heat pump (DSHP), which can utilize either the ambient air or the ground as the heat source or heat sink, the electricity consumption for HVAC can be actively managed so that the electric load profile of a building can be reshaped. Fig. 3 shows a diagram of an integrated DPUTB and DSHP system (referred as "DPUTB-DSHP"). The DPUTB-DSHP system converts electricity to thermal energy (in the form of cold or hot water) with a DSHP and store it in the DPUTB when the renewable power is over-produced, or during the off-peak hours of the grid when the electricity is cheap [Fig. 3(a)]. The stored thermal energy is later utilized to meet buildings' thermal demands with little electricity consumption during peak hours [Fig. 3(b)].

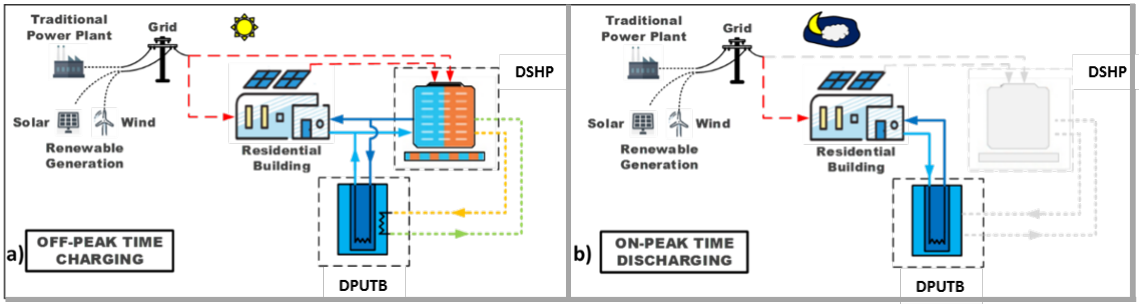

Fig. 3. Schematic of an integrated DPUTB and DSHP system: (a) Condition building and store thermal energy during off-peak hours; (b) Discharge stored thermal energy to reduce electricity consumption during peak hours.

The DPUTB-DSHP system can operate in multiple modes, as shown in Fig. 4. During the off-peak period or when there is an overproduction of renewable power, the DSHP runs at its full capacity. When the ambient temperature is favorable, the DSHP will run as an air source heat pump (ASHP), otherwise it will use the annulus of the DPUTB as a ground heat exchanger and run as a ground source heat pump (GSHP). During this period, if the DSHP's capacity is higher than the thermal demand of the building (Fig. 4a), thermal energy will be stored in the inner tank of the DPUTB. If the DSHP's capacity is lower than the building thermal demand (Fig. 4b), the stored thermal energy in the DPUTB will be discharged to meet the thermal demand. During peak hours, the DSHP is turned off and the stored thermal energy in the DPUTB is used to provide direct cooling/heating to the building (Fig. 4c). Once the stored thermal energy is not enough to meet the thermal demand, the DSHP is switched to GSHP to meet the building thermal demand with high efficiency (Fig. 4d).

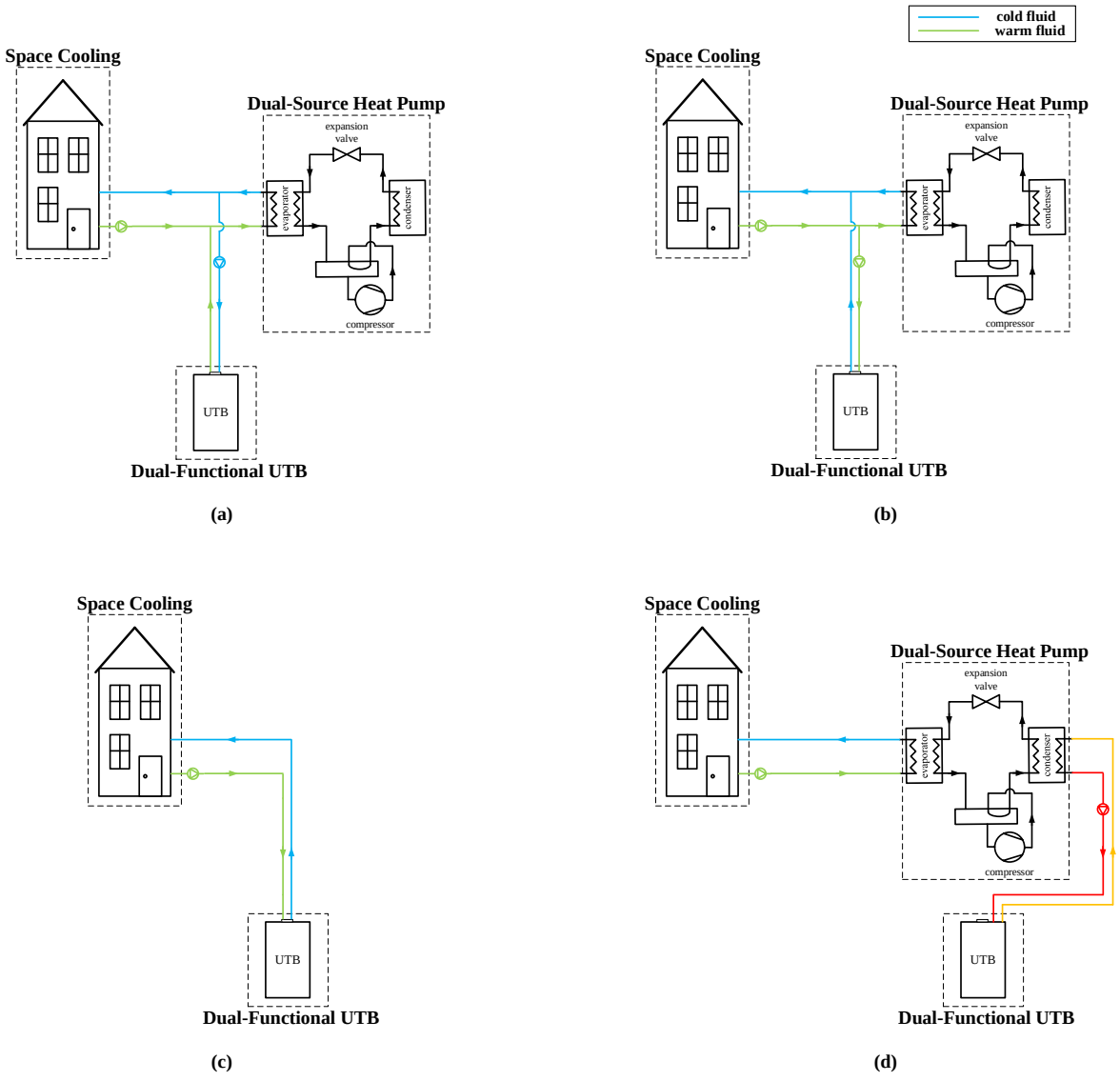

Fig. 4. Multiple operating modes of an integrated DPUTB and DSHP system

2. Model Description

A one-dimensional transient numerical model has been developed to simulate the thermal response of the DPUTB. The model is based on following assumptions and simplifications:

- Only the heat transfer along the radial direction is accounted for;
- Tank water is well mixed due to natural convection, in other words, tank water is isothermal;
- Thermophysical properties of the soil are homogeneous and the heat transfer in the simulation domain is symmetric;
- Convection heat transfer in the liquid PCM is neglected and only the conduction heat transfer is modeled;
- Freezing point of the PCM is identical to its melting point; and
- Heat exchange through the top and bottom surfaces of the DPUTB is neglected.

2.1 Simulation Domain

The simulation domain of the one-dimensional DPUTB model is shown in Fig. 5. The diameter of the simulation domain is 10 time of that of the simulated DPUTB. Because the heat transfer within the soil will not go beyond the boundary for short time periods (e.g., a few months), an adiabatic boundary condition is applied to the perimeter of the simulation domain. The model accounts for following heat transfer processes:

- Heat transfer between the heat exchanger in the inner tank (HEX1) and the inner tank water;
- Heat transfer between the heat exchanger in the outer tank (HEX2) and the outer tank water;
- Heat transfer between the inner and outer tank water through the inner tank wall (made with PVC) and the PCM wrapped around the inner tank;
- Heat transfer between the DPUTB shell and the surrounding soil;
- Phase change process within the PCM; and
- Phase change process within the inner tank.

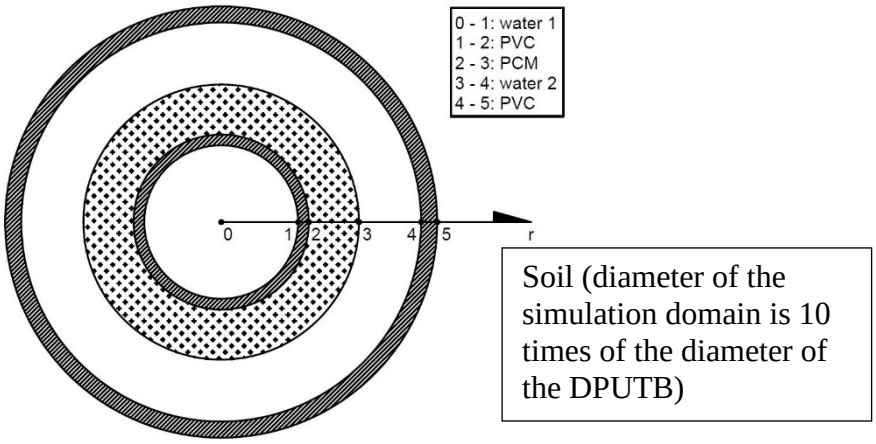

Fig. 5. Simulation domain of the one-dimensional model of DPUTB

2.2 Governing Equations

2.2.1 Heat exchanger modeling

HEX1 and HEX2 are heat exchangers directly interact with the inner and outer tank water. Given their UA values, inlet temperatures, and mass flows, the input thermal energy to the tank water can be determined.

The heat exchange rate between the tank water and the heat exchanger is calculated with Eq. 1:

$$q = UA \cdot \Delta T_{lm} \tag{1}$$

where, q is the heat exchange rate, U is the heat transfer coefficient of the heat exchanger, A is the surface area of the heat exchanger, and ΔT_{lm} is the logarithm mean temperature difference between the fluid in the heat exchanger and the tank water at a given time step, which is expressed as (Eq. 2):

$$\Delta T_{lm} = \frac{(T_{HEX,in} - T_{tank}) - (T_{HEX,out} - T_{tank})}{\ln \frac{T_{HEX,in} - T_{tank}}{T_{HEX,out} - T_{tank}}} \tag{2}$$

where, $T_{HEX,in}$ is the inlet temperature of the heat exchanger, $T_{HEX,out}$ is the outlet temperature of the heat exchanger, and T_{tank} is the tank water temperature.

At steady state, the heat exchange rate is also equal to the enthalpy change of the fluid in the heat exchanger, which can be calculated with Eq. 3:

$$q = \dot{m}_{HEX} \cdot c_p \cdot \left(T_{HEX,in} - T_{HEX,out}\right) \tag{3}$$

where, $\dot{m}_{HEX}$ is the mass flow of the heat carrier fluid in the heat exchanger, and c_p is the specific heat of the heat carrier fluid.

Therefore, the above equations are solved iteratively to determine the heat exchanger outlet temperature and the heat transfer rate at a given time step. The calculated heat transfer rate is used as a boundary condition of the DPUTB model.

2.2.2 Natural convection modeling

In order to determine the convection heat transfer coefficient between the tank water and its surrounding solid surfaces, the Rayleigh number and the Nusselt number are calculated with Eq. 4 and Eq. 5, respectively:

$$\mathrm{Ra} = \frac{g \cdot \beta \cdot |T_s - T_\infty| \cdot L^3}{\nu \cdot \alpha} \tag{4}$$

where, g is the gravity, β is the coefficient of thermal expansion of the fluid, T_s is the surface temperature, T_∞ is the fluid bulk temperature, L is the characteristic length, ν is the kinematic viscosity, and α is the thermal diffusivity of the fluid.

$$\mathrm{Nu} = \left\{ 0.825 + \frac{0.387 \cdot \mathrm{Ra}^{\frac{1}{6}}}{\left[1 + (0.492/Pr)^{\frac{9}{16}}\right]^{\frac{8}{27}}} \right\}^2 \tag{5}$$

where, Pr is the Prandtl number of the fluid.

The convective heat transfer coefficient can be determined with Eq. (6):

$$h_{conv} = \mathrm{Nu} \cdot \frac{k}{L} \tag{6}$$

where, k is the thermal conductivity of the fluid.

The surface temperature can be calculated based on the energy balance at the surface:

$$h_{conv} \cdot (T_\infty - T_s) = \frac{k_{other}}{\Delta x} \cdot (T_s - T_{other}) \tag{7}$$

where, k_{other} is the thermal conductivity of the material on the other side (either PCM or tank wall).

The above equations (4) through (7) are solved iteratively to determine the surface temperature of the solid surface at a given time step.

2.2.3 Conduction heat transfer

The PCM and soil are discretized into a series of small cells along the radial direction and conduction heat transfer equation is applied to each cell to determine its average temperature. For one-dimensional heat conduction in the cylindrical coordinates, the conduction heat transfer equation can be expressed as Eq. (8):

$$\frac{1}{r}\frac{\partial}{\partial r}\left(r \cdot k \frac{\partial T}{\partial r}\right) = \rho \cdot c_p \frac{\partial T}{\partial t} \tag{8}$$

where, r is the radial position of the cell, and ρ is the density of the material within the cell.

For explicit numerical calculation, the heat equation can be discretized into the following expression, as expressed in Eq. (9):

$$\rho \cdot c_p \frac{T_i^{new} - T_i}{\Delta t} = \frac{1}{r_i} \cdot \frac{r_{i+\frac{1}{2}} \cdot k_{i+\frac{1}{2}} \frac{T_{i+1} - T_i}{\Delta r} - r_{i-\frac{1}{2}} \cdot k_{i-\frac{1}{2}} \frac{T_i - T_{i-1}}{\Delta r}}{\Delta r} \tag{9}$$

where, the subscripts denote the position and the superscripts denote the time step. Applying this equation to each cell gives the temperature profile of the soil and PCM at a given time step.

2.2.4 Phase change modeling

The latent heat accumulation method (Muhieddine et al., 2009) is applied to simulate the phase change process within the PCM and the inner tank (filled with water or another PCM). During the phase changing period, the temperature of the PCM is fixed but the latent heat within the PCM mass is changing. For certain amount of PCM, the maximum latent heat it can store can be calculated as:

$$Q_{latent,max} = m \cdot \Delta H \tag{10}$$

where, m is the mass of the PCM, and ΔH is the heat of fusion.

If the PCM is in solid or liquid phase, there is no latent heat involved in the heat transfer process. When a PCM cell (finite control volume) is frozen (i.e., from liquid to solid), a parameter 'solid fraction' is defined based on how much latent heat is accumulated, and it is expressed with Eq. 11:

$$\theta = 1 - \frac{Q_{latent,acc}}{Q_{latent,max}} \tag{11}$$

where, θ is the solid fraction, and $Q_{latent,acc}$ is the amount of latent heat accumulated in the finite control volume. According to this definition, if the cell is all in solid phase, $\theta = 1$; and if the cell is all in liquid phase, $\theta = 0$. When the cell is in two-phase, θ ranges between 0 and 1, and it reflects how much solid is in the cell.

Within each time step, after the heat equation calculation, the phase status of each cell is checked. Four possible scenarios can happen: two-phase melting, two-phase freezing, single phase solid, and single phase liquid. If the cell is in two-phase, tag the cell for further time step calculation. Take the melting scenario as an example: if the cell is tagged in melting, the cell temperature is reassigned to the melting temperature and the latent heat increment is calculated from the fictitious sensible heat. The fictitious sensible heat is added to the accumulated latent heat storage of the cell for subsequent time steps until the accumulated latent heat equals the maximum latent heat available in the control volume. At this time step, the control volume becomes all liquid, the tag on the cell is removed and the latent heat increment is no longer calculated. The freezing scenario is of the same principle and only the latent heat is inverted from storing to releasing.

2.3 Computational Method

The explicit method is applied to solve the discretized heat transfer equations at each time step based on the temperature profiles of the soil and the PCM domains in the last time step and tank water temperatures at the current time step. The explicit method is easy to conduct but a certain stability confinement, expressed with Eq. (12) should be satisfied:

$$d = \frac{\alpha \cdot \delta t}{(\delta r)^2} \leq 0.5 \tag{12}$$

where, $\boldsymbol{d}$ is the stability determinant, $\boldsymbol{\alpha}$ is the thermal diffusivity of the material, $\boldsymbol{\delta t}$ is the time increment, and $\boldsymbol{\delta r}$ is the radius increment of the cell.

3. Model Validation

A small-scale prototype of DPUTB was built at the Oak Ridge National Laboratory. The dimensions of the small-scale DPUTB prototype are listed in Table 1, along with the thermal properties of the PCM used in the prototype. The DPUTB prototype was tested in a chamber with controlled climate. For the first six hours the inner tank water was charged with an coolant (mixture of water and glycol) at around 0 °C. In the following two hours, the inner tank was heated up using HEX 1 to emulate the discharging scenario. In the last seven hours HEX 1 was turned off and heat was rejected to the annulus of the DPUTB intermittently through HEX 2 to emulate the operation of a GSHP.

The lab test results were used to validate the numerical model. For the current validation, three parameters—the ambient temperature, inlet temperatures from HEX1, and inlet temperatures from HEX2—were applied as the boundary conditions. The mass flow rates of HEX1 and HEX2 were constant during the whole experiment period, and their values were 26.5 kg/h. The UA values (i.e., the product of the heat transfer coefficient and the surface area) of the two heat exchangers are difficult to quantify due to the complicated geometry of the helical coil heat

exchangers used in the prototype; therefore, it was estimated based on the typical UA value (5,000 W/°C) for similar heat exchangers. With the abovementioned data as inputs of the numerical model, the model predictions and the experimental data show similar trends. However, the model predicted a lower inner tank water temperature during the first and third periods. It indicates that the model overestimates the insulation effect between the inner and outer tanks. The most plausible reason for this overestimation is that the PCM applied in the experiment consisted of three layers of commercially available PCM panels instead of the ideal one layer of PCM defined in the model. It is likely that some water flowed between the PCM panels in the lab test, which enhanced heat transfer. The enhanced heat transfer is equivalent to a much higher thermal conductivity of the PCM. Figures 6 and 7 show the comparison results after increasing the thermal conductivity of the PCM in the model from 0.15 to 0.60 W/m K. The simulation results resulting from increased thermal conductivity value of the PCM match well with the experimental data. The root square means error for the inner tank water temperature is 0.4°C, and for the outer tank water temperature is 0.8°C. It indicates that the numerical model can predict the performance of a DPUTB with reasonable accuracy.

Table 1. Dimensions and thermal properties of the small-scale DPUTB prototype

Dimension	Value	Unit	PCM properties	Value	Unit
Inner tank diameter	7.79	cm	Melting point	23	°C
Inner PVC shell thickness	0.55	cm	Heat of fusion	160	kJ/kg
PCM blanket thickness	2.54	cm	Thermal conductivity (solid)	0.1489	W/m K
Outer tank diameter	20.27	cm	Thermal conductivity (liquid)	0.1596	W/m K
Outer PVC shell thickness	0.82	cm	Specific heat (solid)	3000	J/kg K
Height of the inner tank	121.92	cm	Specific heat (liquid)	2740	J/kg K
Height of the outer tank	121.92	cm			

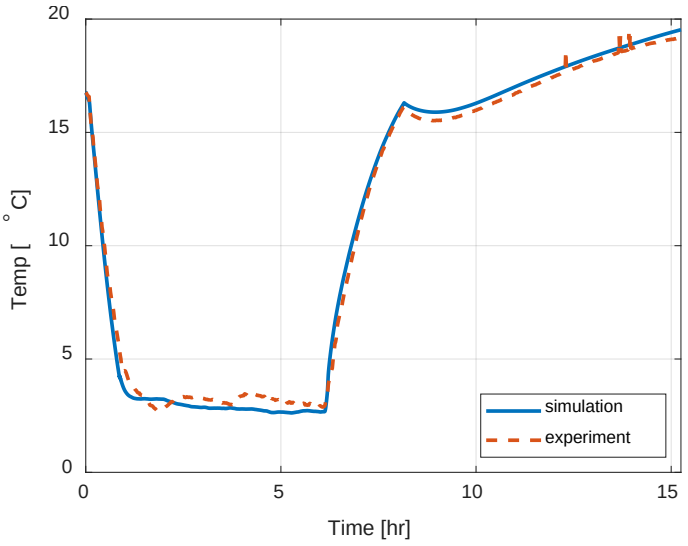

Figure 6. Comparison between measured and model-predicted inner tank water temperature of the small-scale prototype DPUTB (with increased thermal conductivity of PCM to account for possible water flow between the PCM sheets).

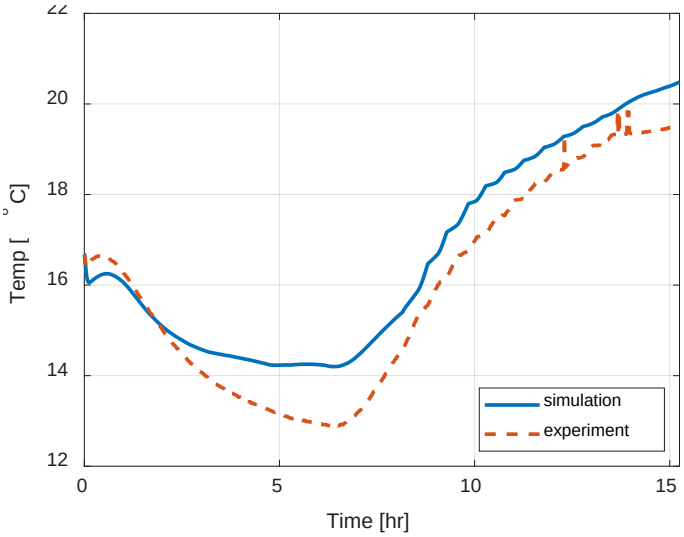

Figure 7. Comparison between measured and model-predicted water temperature in the annulus of the small-scale prototype DPUTB (with increased thermal conductivity of PCM to account for possible water flow between the PCM sheets).

4. Simulation Results of DPUTB Integrated Heat Pump

4.1 System Configuration

Fig. 8 shows the diagram of the simulated DPUTB-DSHP system. The refrigerant discharged from the DSHP's compressor can go to either a direct expansion condenser unit (i.e., a conventional air-water heat pump [AWHP]) or a coaxial coil heat exchanger (i.e., a conventional water-water heat pump [WWHP]), which is then connected with the helical heat exchanger in the annulus of the DPUTB. The chilled water (7°C) produced at the DSHP's evaporator is supplied to the building's HVAC system and the heat exchanger in the DPUTB's inner tank using a constant speed pump (P1). The DPUTB can be charged with the chilled water to store cooling energy with the PCM in the inner tank (by opening valves 1 and 4 and closing valves 2 and 3) or can be discharged to provide cold water to the building HVAC system (by opening valves 2 and 3 and closing valves 1 and 4). During the discharging operation, a variable speed pump (P2) dedicated to the DPUTB is operated to provide chilled water as needed for meeting the building's varying cooling loads. Another pump (P3) is used to circulate water between the DSHP's coaxial heat exchanger and the heat exchanger in the DPUTB's annulus. It is assumed that the leaving fluid temperature of the HVAC terminals in the building is maintained at 14°C.

The experimentally validated DPUTB model is incorporated with a simplified model for the DSHP to simulate the operation of a DPUTB-DSHP system. The DSHP is modeled as a combination of two conventional heat pumps: an AWHP and a WWHP. Two curve fitting submodels were based on the heat pump models (type 927 and type 941) of the TRNSYS program (Klein et al. 2017). These heat pump models use performance curves of typical AWHP and WWHP units to predict their heating and cooling output and associated power consumption based on the inlet conditions at the condenser and the evaporator of these heat pumps.

In this case study, the maximum cooling capacity of the DSHP is 1.45 ton. It is assumed that DSHP uses a variable speed compressor so that it can adjust its cooling capacity based on control signals. The key parameters of the simulated DPUTB are listed in Table 2.

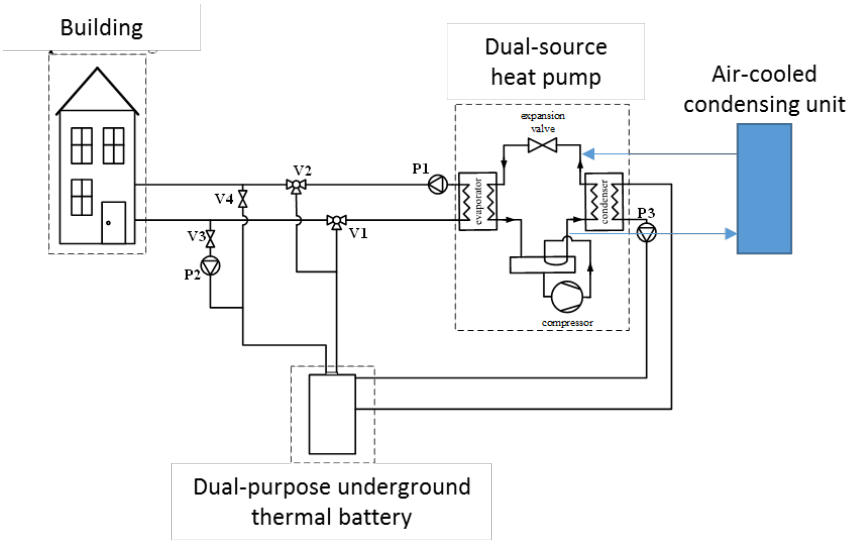

Fig. 8. Diagram of the modeled DPUTB-DSHP system.

Table 2. Dimensions and key properties of the simulated dual-purpose underground thermal battery

Property	Value	Unit
DPUTB dimensions		
Inner tank diameter	39	cm
Inner PVC shell thickness	0.55	cm
PCM blanket thickness	2.54	cm
Outer tank diameter	101.37	cm
Outer PVC shell thickness	0.82	cm
Height of the inner tank	609.60	cm
Height of the outer tank	609.60	cm
Inner shell thermal physical properties		
Material	PVC	–
Thermal conductivity	0.19	W/m K
Density	1380	kg/m^3
Specific heat	1000	J/kg K
Outer shell thermal physical properties		
Material	HDPE	–
Thermal conductivity	0.50	W/m K
Density	950	kg/m^3
Specific heat	1900	J/kg K
Inner tank PCM thermal physical properties		
Melting point	12	°C
Heat of fusion	334	kJ/kg
Density (solid)	917.5	kg/m^3
Density (liquid)	998	kg/m^3
Thermal conductivity (solid)	2.25	W/m K

Table 2. Dimensions and key properties of the simulated dual-purpose underground thermal battery (continued)

Property	Value	Unit
Thermal conductivity (liquid)	0.6	W/m K
Specific heat (solid)	2027	J/kg K
Specific heat (liquid)	4182	J/kg K
Annulus PCM thermal physical properties		
Melting point	14	°C
Heat of fusion	160	kJ/kg
Density	1118	kg/m^3
Thermal conductivity (solid)	0.1489	W/m K
Thermal conductivity (liquid)	0.1596	W/m K
Specific heat (solid)	3000	J/kg K
Specific heat (liquid)	2740	J/kg K
Soil thermal physical properties		
Thermal conductivity	1.70	W/m K
Density	1602	kg/m^3
Specific heat	2100	J/kg K

The hourly cooling load of a residential building in Baltimore, MD was predicted with the US Department of Energy's (DOE's) prototype model for residential building, a single-family detached house (DOE 2014). The hourly cooling load is used as an input to the system simulation. The prototype residential building uses a conventional HVAC system, which includes an air conditioner with a nominal coefficient of performance (COP) of 3.97 and a gas furnace with an efficiency of 0.78. The electric load profile and power consumption of the prototype residential building were used as a baseline to be compared with that resulting from using the DPUTB-DSHP system.

4.2 Control Strategy

The control strategy of the DPUTB-DSHP system is shown in Fig. 9, and descriptions of various operating modes are listed in Table 3. The operation mode at a given time is determined with the following procedures depending on whether the current time is on-peak or off-peak.

- If current time is on-peak, check whether the DPUTB inner tank water temperature is lower than the melting point of the PCM inside the inner tank.
  - If so, only use the stored cooling energy in the DPUTB to meet the cooling demand of the building (mode 7).
  - If not, check whether the ambient air temperature is lower than 26.7 °C.
    - If yes, operate DSHP as ASHP to meet the cooling demand (mode 1).
    - Otherwise, operate DSHP as a GSHP to meet the cooling demand (mode 4).

- If current is off-peak, operate DSHP as an ASHP if the ambient air temperature is lower than 26.7°C, otherwise operate DSHP as a GSHP.

- In each case (ASHP or GSHP), check whether the DPUTB is fully charged.
  - If yes, operate DSHP to meet the cooling demand (mode 1 or mode 4).
  - Otherwise, check whether the cooling demand is lower than the cooling capacity of the DSHP.
    - If yes, run DSHP to meet the cooling demand and charge DPUTB (mode 2 or mode 5).
    - Otherwise, run DSHP at its maximum capacity and together with discharging DPUTB to meet the cooling demand (mode 3 or mode 6).

The cooling capacity of the DSHP is adjusted at each time step based on the difference between the targeted whole building electric demand and the sum of the electric demands of all the non-HVAC end uses in the building at the time step. The difference in the electric demand is the allowed power draw of the DSHP, which can be translated to the allowed cooling capacity of the DSHP at the time step based on the efficiency of the DSHP. It is assumed that when the allowed cooling capacity of the DSHP is lower than 55% of its maximum capacity, the DSHP is turned off, and the building's cooling demand is met solely by the stored cooling energy in the DPUTB.

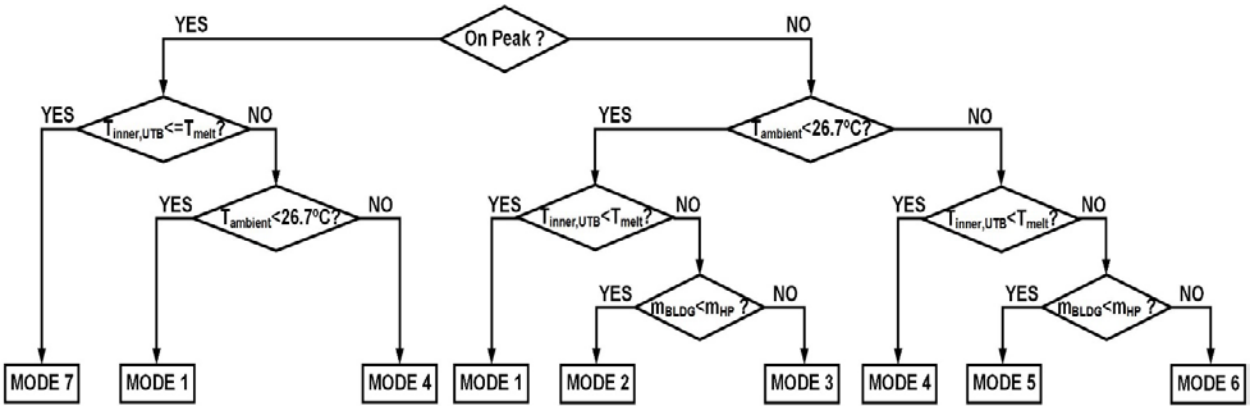

Fig. 9. Strategies for determining the operation mode of the DPUTB-DSHP

Table 3. Description of each operating mode of the integrated heat pump and thermal energy storage system

Mode	Description
1	Heat pump on (air source), DPUTB off
2	Heat pump on (air source), DPUTB charging
3	Heat pump on (air source), DPUTB discharging
4	Heat pump on (ground source), DPUTB off
5	Heat pump on (ground source), DPUTB charging
6	Heat pump on (ground source), DPUTB discharging
7	Heat pump off, DPUTB discharging

4.3 Simulation Results

The simulation results on a typical summer day (July 21) are shown in figs. 10 through 12. Fig. 12 clearly shows that the building's electric load profile is flattened by DPUTB-DSHP system. Compared with the electric load profile resulting from using the conventional HVAC system, the

DPUTB-DSHP system reduces the peak electric demand during peak hours—from 10:00 to 20:00 (Baltimore Electric and Gas Company 2018)—by 37%. The DPUTB-DSHP system operates in the following different modes during the day:

- From 0:00 to 10:00, because of the relatively low ambient temperature, the DSHP operates as an ASHP to provide space cooling to the building and charge the DPUTB in the meanwhile. As shown in Fig. 11, the solid fractions of the PCMs in both the inner tank and annulus are increasing (i.e., the PCMs are frozen) during this period. On the other hand, the water temperature in the annulus barely changes due to the insulating effect of the PCM wrapping around the inner tank. Fig. 11 shows that the capacity fraction of the DSHP (indicated by the dotted yellow line) ranges from 70% to 100% of its maximum capacity.

- From 10:00 to 14:00, the DPUTB is still being charged while the DSHP switches to GSHP (i.e., rejecting heat to the annulus of the DPUTB) because the ambient air temperature is higher than the threshold (26.7°C). Due to heat rejection from the DSHP, the water temperature of the annulus increases, and the slopes of the solid fraction of the PCMs decrease. The capacity fraction of the DSHP is maintained at 80% as shown in Fig. 12.

- From approximately 14:00 to 17:00, the building's cooling demand exceeds the maximum cooling capacity of the DSHP. Therefore, the DPUTB is discharged to release some cooling energy (indicated by the negative values of the blue line in Fig. 12). The capacity fraction of the DSHP later drops from 80% to 55% due to the decreasing cooling demands.

- From 17:00 to 23:00, the DSHP is turned off, and the DPUTB releases stored cooling energy to meet the building's cooling demand. The solid fractions of the PCMs decrease as the stored cooling energy is released from the PCMs. The water in the annulus of the DPUTB is cooled by the surrounding soil (Fig. 11).

- After 23:00, the capacity fraction of the DSHP increases above 55%, and the ambient temperature is lower than 26.7°C, so the DSHP runs as an ASHP again to provide space cooling to the building and charge the DPUTB as it does in the first period.

In addition to reducing the peak electric demand, the DPUTB-DSHP system reduces the building's power consumption by 11% (from 4.47 kWh to 3.99 kWh) compared with baseline results using the conventional HVAC system. The energy savings results from the more efficient operation of the GSHP when the ambient air temperature is high. The GSHP's average operational efficiency, indicated by the COP, was ~6 when operating. The results of this case study indicate that the DPUTB-DSHP system can effectively shift the electric load while reducing the power consumption of the simulated residential building.

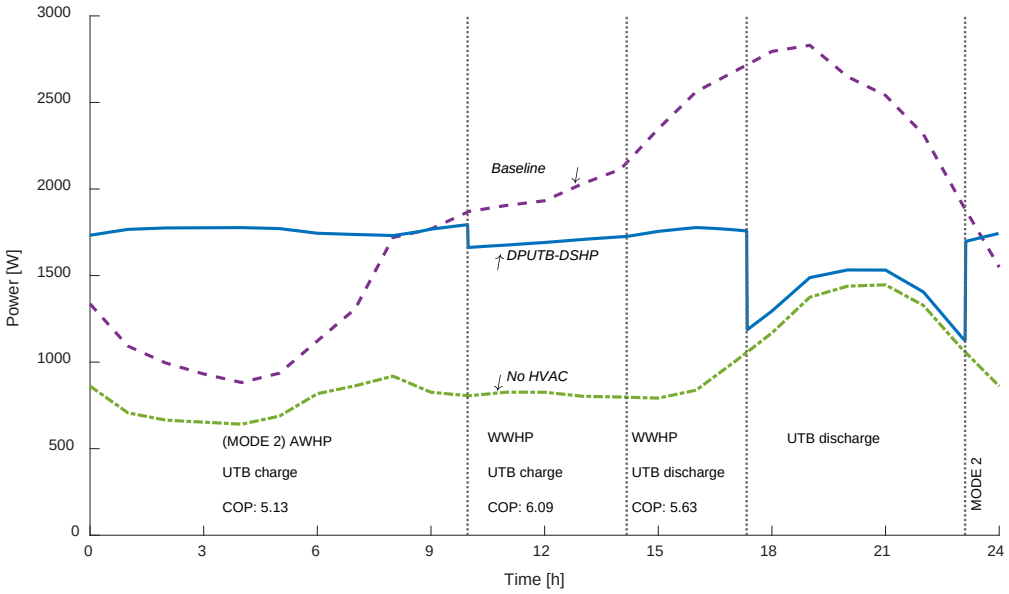

Fig. 10. Electric load profile of the building

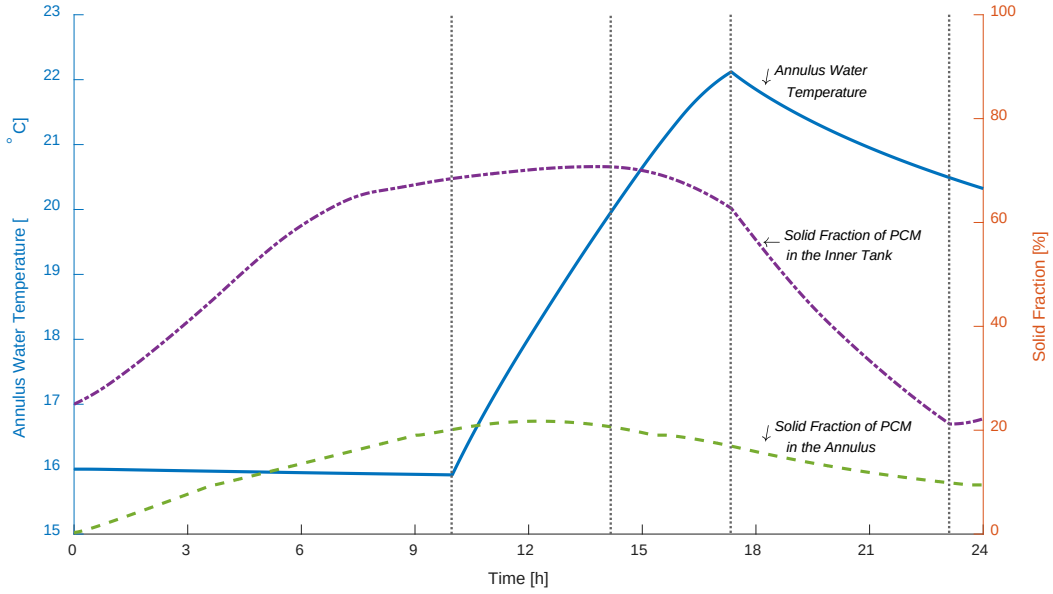

Fig. 11. Water temperature in the annulus of the DPUTB and the solid fractions of PCMs in the inner tank and the annulus of the DPUTB

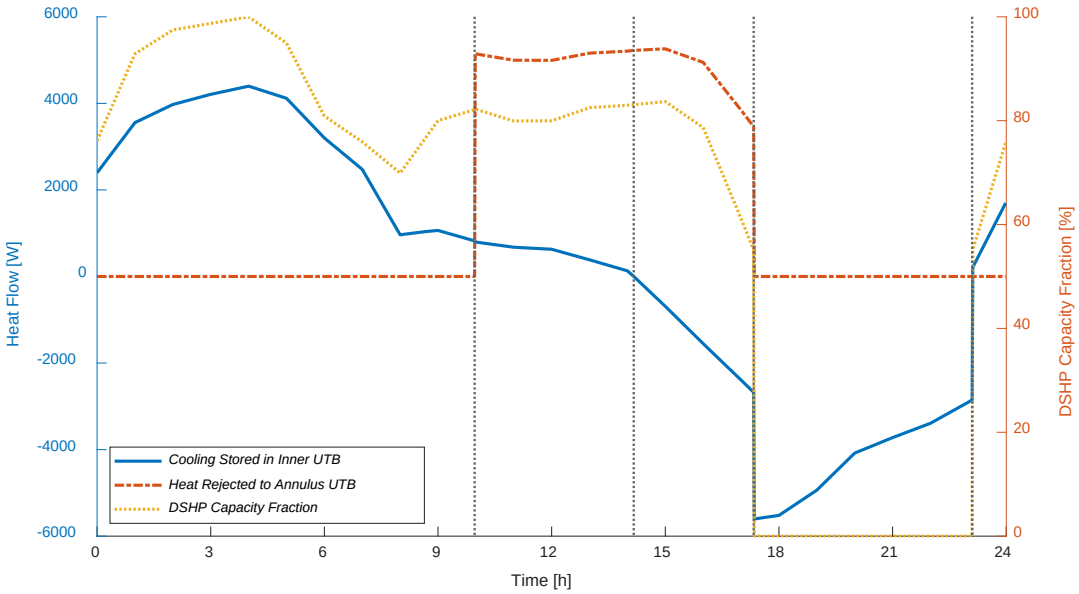

Fig. 12. Thermal loads of the DPUTB in the inner tank and the annulus and the capacity fraction of the DSHP

5. Conclusions and plan for future work

A one-dimensional transient numerical model of a novel thermal energy storage system, the dual-purpose underground thermal battery (DPUTB), has been developed and validated against the measured performance data of a small-scale prototype of DPUTB. The validated DPUTB model was incorporated into a heat pump system simulation to predict its performance under various operating conditions of a typical residential building in the United States. The simulation results indicate that the DPUTB-DSHP system can shift or level the electric load profile of a typical residential building. Besides, the DPUTB also provides a low-cost ground heat exchanger, which enables highly efficient operation of a GSHP to meet the thermal demands of the building. As a result, the DPUTB-DSHP system not only significantly reduces the building's electric demand during peak hours, but also saves energy compared with conventional HVAC systems. When deployed at large scale, this system could help mitigate the growing burden on the nation's electric grid, especially the duck-curve effect that results from increasing penetration of intermittent renewable power generation.

Following research and development work is recommended to get further understanding on the benefits and costs of the DPUTB integrated heat pump systems:

- Improve the numerical model of DPUTB to account for seasonal variation of the soil temperature and heat fluxes on the ground surface.
- Further develop the system simulation to investigate the performance of the system for heating operation. The configuration and size of the DPUTB, as well as the control

strategy of the DPUTB integrated heat pump system need to be tailored for the heating operation.

- Evaluate long-term (e.g., seasonal or annual) performance of the DPUTB integrated heat pump system. Particularly, investigating the impact of thermal build-up in the surrounding soil of the DPUTB.
- Assess the benefits and costs of the DPUTB integrated heat pump system and compare it with other thermal energy storage systems for shifting electric demands of buildings.
- Optimize DPUTB design and its integration with the heat pump system to maximize cost effectiveness.

Acknowledgement

This work was sponsored by the U. S. Department of Energy's Geothermal Technologies Office under Contract No. DE-AC05-00OR22725 with UT-Battelle, LLC. The authors would also like to acknowledge Ms. Arlene Anderson and Joshua Mengers, U.S. Department of Energy Geothermal Technologies Office.

REFERENCES

Baltimore Gas and Electric Company (2018). Residential Optional Time-Of-Use – Electric Schedule RL. CAISO (2013) What the Duck Curve Tells us about Managing a Green Grid. https://www.caiso.com/Documents/2011-08-10_ErrataLTPPTestimony_R10-05-006.pdf

Klein, S.A. et al, 2017, TRNSYS 18: A Transient System Simulation Program, Solar Energy Laboratory, University of Wisconsin, Madison, USA, http://sel.me.wisc.edu/trnsys.

https://www.bge.com/MyAccount/MyBillUsage/Documents/Electric/P3_SCH_RL.pdf

NREL (2015). Overgeneration from Solar Energy in California: A Field Guide to the Duck Chart. https://www.nrel.gov/docs/fy16osti/65023.pdf

U.S. Energy Information Administration (2018). Annual Energy Outlook 2018.

Muhieddine, M., Canot, E., & March, R. (2009). Various approaches for solving problems in heat conduction with phase change. International Journal on Finite Volumes, 19.

U.S. Department of Energy (2014). Building Energy Codes Program: Residential Prototype Building Models. Retrieved from https://www.energycodes.gov/development/residential/iecc_models